THE AMERICAN MINERALOGIST, VOL. 50, JANUARY–FEBRUARY, 1965

STUDIES ON THE FORMATION OF CRYSTALLINE SYNTHETIC BROMELLITE. I. MICROCRYSTALS[1]

HERBERT W. NEWKIRK AND DEANE K. SMITH, *Lawrence Radiation Laboratory, University of California, Livermore, California.*

ABSTRACT

Synthetic bromellite (BeO) microcrystals have been grown by (1) oxidation of beryllium in wet hydrogen at 1525° C., (2) water-vapor attack on polycrystalline BeO at 1525° C., and (3) from lead fluoride (PbF_2)-BeO mixtures at 925° C. The microcrystals are of two types, whiskers and platelets. Three types of whiskers have been observed, depending on whether the growth direction is $[00\cdot1]^*$, $[1\bar{1}\cdot0]^*$, or $[10\cdot0]^*$. The first type is the most common, and in the presence of PbF_2 it is the only type observed. The larger whiskers of this type are often hollow, but electron microscopy does not verify the existence of cores in the smaller ones. Water vapor attack produces all three types of whiskers. The $[10\cdot0]^*$ type is very rare and was not observed among whiskers overgrown on single crystal substrates. Overgrown whiskers are similar to the smaller as-grown whiskers, and do not contain pores, are not twisted, and appear smooth at magnifications to 100,000×. Some whiskers obtained from PbF_2-BeO mixtures are as long as 10 cm, can be stressed to 3,000,000 lb/in² in bending, and elastically strained 4.5%. Axial growth rates were 0.1 μ/sec in methods (1) and (2) and 0.4–1.3 μ/sec in method (3). Plausible growth mechanisms are described for some of the various types of whiskers grown.

Platelets are of three types formed by growth along the combinations of two of three whisker directions. The most common platelets are the $[00\cdot1]^*$-$[1\bar{1}\cdot0]^*$ type. Twinning was frequently observed with either the $(11\cdot2)$ or the $(10\cdot3)$ as the twin plane. The relationship of the structures across the twin boundaries and their strong tendency to twin on these planes was interpreted with respect to the polar crystal structure. A growth mechanism is discussed for the $(10\cdot3)$ twinned platelets.

INTRODUCTION

The mineral bromellite, named after the Swedish physician and mineralogist Magnus von Bromell (1670–1731), occurs as 1-mm-long prismatic crystals in a limited area around Langban, Sweden. The mineral analyzes 98.02% BeO, 1.03% CaO, 0.55% BaO, 0.97% MgO with traces of MnO, Sb_2O_5 and Al_2O_3. Because of its scarcity and low purity there has been great emphasis during recent years in developing a high purity synthetic compound.

Synthetic bromellite (BeO) is finding wide application not only in high-temperature refractory ware but also as a moderator in gas-cooled nuclear reactors and as a dielectric in electronic applications. The growth of flawless crystals is a prime prerequisite for determining the fundamental properties of this technologically useful and interesting material.

The results of our growth studies are reported in two papers. This paper discusses the growth of microcrystals and the following paper treats the

[1] Work performed under the auspices of the U. S. Atomic Energy Commission.

growth of macrocrystals. In each paper, the relationship between the growth mechanisms, habits, and twinning phenomenon involved in the synthesis are discussed in detail and correlated with the polar-crystal structure.

Microcrystals were grown by oxidizing beryllium, decomposing beryllium hydroxide vapor, and by hydrolyzing gaseous beryllium fluoride at elevated temperatures. Observations as to variations in morphology, growth directions, twinning and kinking, surface features, and bending strengths have been recorded. *X*-ray diffraction, electron microscopy and diffraction, and interference and optical microscopy have all been used to study the crystals. Ultimate strength was measured by bending microcrystals to failure and observing the radius of curvature near failure.

Experimental Results

Growth. Synthetic bromellite microcrystals were grown by oxidizing beryllium, decomposing beryllium hydroxide vapor, and by hydrolyzing gaseous beryllium fluoride at elevated temperatures. Growth by the oxidation of beryllium powder (99.9+% beryllium) was accomplished using a BeO boat to contain the powder in an alumina tube furnace with a flowing hydrogen atmosphere at 1525° C. for 16 h. The hydrogen entering the furnace had a partial pressure of water of 0.01 mm Hg. The spent gas contained a partial pressure of water of 0.03 mm Hg. The probable reactions occurring are, first, the generation of water vapor and gaseous aluminum oxide species by hydrogen reduction of the alumina tube according to the equation

$$1/2\ Al_2O_3(s) + H_2(g) = 1/2\ Al_2O(g) + H_2O(g),$$
$$\Delta F^\circ = +\ 61\ \text{kcal/mole}. \qquad (1)$$

Second, the products resulting from equation (1) then react with beryllium to form the oxide by either or both of the reactions

$$Be(l) + H_2O(g) = BeO(s) + H_2(g),$$
$$\Delta F^\circ = -\ 65\ \text{kcal/mole} \qquad (2)$$

or

$$Be(l) + 1/2\ Al_2O(g) = 1/2\ BeO(s) + Al(l),$$
$$\Delta F^\circ = -\ 15\ \text{kcal/mole}. \qquad (3)$$

The water vapor may also react with the BeO boat to form the volatile hydroxide by the reaction

$$BeO(s) + H_2O(g) = Be(OH)_2(g),$$
$$\Delta F^\circ = +\ 30\ \text{kcal/mole}. \qquad (4)$$

Since the boat and its contents were heated nonisothermally, reaction (4) will reverse in cooler portions of the furnace. The observed average growth

rates were 0.1 μ/sec and the growth of BeO microcrystals occurred throughout the interior of the boat.

Growth by decomposing beryllium hydroxide vapor, according to equation (4), was carried out in a more direct fashion as follows: a dense polycrystalline BeO cylinder (99.9+% BeO) was placed in the hottest section of an alumina tube furnace. Single-crystal or dense non-orientated polycrystalline BeO substrates were placed downstream from the nutrient in a lower temperature zone. The BeO nutrient and substrates were heated in a flowing, water-saturated helium atmosphere for 24 h. The nutrient zone was held at 1525° C. and growth occurred on the substrates at 1400° C.

In the third technique, a 100-g charge of lead fluoride (99.9+% PbF_2) powder was placed in a 250-ml platinum container together with a dense polycrystalline BeO rod, 1.25 cm in diameter and 7.5 cm long. The rod, which serves both as the reacting material and as the substrate, was supported upright in the center of the container by wires. A loosely fitted cover was placed over the container, and the assembly was heated in an electric oven with air for 12 h at 925° C. The quantity of PbF_2 was such that the BeO rod was only partially immersed in liquid and was sufficient to give a good yield of whiskers at average growth rates of 0.4–1.3 μ/sec. The important vapor-phase chemical reactions involved in this synthesis are described by the following equations:

$$\begin{aligned} PbF_2(g) + BeO(s) &= BeF_2(g) + PbO(l), \\ \Delta F^\circ &= -12 \text{ kcal/mole} \end{aligned} \tag{5}$$

and

$$\begin{aligned} BeF_2(g) + H_2O(g) &= BeO(s) + 2HF(g), \\ \Delta F^\circ &= +32 \text{ kcal/mole.} \end{aligned} \tag{6}$$

When BeF_2 powder was used as the starting material, microcrystals did not form, but, instead, large crystals grew on the lid of the platinum container at the point where vapors evolved to the atmosphere. The growth and morphology of these crystals are described in the following paper.

Morphology. The microcrystals are of two general habits: filaments and platelets. All the methods produced whiskers, but the platelets were obtained only by oxidizing beryllium metal.

Three types of whiskers have been identified. The classification is based on the crystallographic orientation of the fiber or growth axis. Using single crystal x-ray diffraction techniques, these axes have been identified in the order of abundance as $[00\cdot1]^*$, $[1\bar{1}\cdot0]^*$, and $[10\cdot0]^*$ and will be referred to as types C, A2, and A1, respectively. Type A1 corresponds to

the type-I whisker reported by Edwards and Happel (1963); the A2 whisker is the whisker described by Scott (1959). The type-A1 whisker was found to be rare in this study. Type-II whiskers, as described by Edwards and Happel (1963), growing along [30·2], were never observed in any of our experiments, and attempts to duplicate their experiments were unsuccessful.

The type-C whiskers are common regardless of growth conditions. Usually these crystals are well formed with hexagonal cross sections bounded by the first-order prism {10·0}. Even at magnifications as high as 100,000×, most prismatic surfaces are smooth. Occasionally crystals taper along their length to a very sharp point by the alternation of a pyramidal form with the prism. The optical properties, such as the interference figure, indices of refraction, and birefringence are those of BeO, uniaxially positive with $\omega = 1.719$ and $\epsilon = 1.733$. Sometimes they may have a hollow core along about one-half the length of the crystal. This core is usually tapered and appears to indicate "hopper" or dendritic growth of the crystal. This growth characteristic appears only in the presence of fluoride ions. The type-C whiskers showed no evidence of twisting nor were any cores observed running the full length of the crystal even at high magnifications under the electron microscope.

Type-A2 whiskers are most abundantly formed by the decomposition of $Be(OH)_2$. The whiskers were found to be smooth at magnifications to 100,000× and were not cored or twisted. At high magnifications in the electron microscope complex arrays of lines of strong contrast were observed within some of these microcrystals. These extinction line contours are normally attributed to elastic buckling or bending of the whiskers and indicate an inherent strain field in the whisker (Lasko and Tice, 1962). Attempts to associate these lines with a strain field induced by a lattice defect in the whisker were not successful but are a subject of continuing study. Figure 1a shows branching of A2 whiskers to form type-C whiskers and vice versa. This complex array of fibers apparently has only one crystallographic orientation as indicated by x-ray diffraction. Figure 1b shows one cluster of fibers looking along the [00·1]* direction. Many 60° kinks are present, but no 30° kinks to type-A1 whiskers have been observed. The orientation of some of the fibers has been verified by x-ray diffraction.

As already stated, type-A1 whiskers are rare. A few were found among the crystals formed by oxidation of Be metal. In general most of the type-A1 whiskers develop into platelets which will be described below.

In one series of experiments, single crystals of BeO were used as a substrate for oriented overgrowth. Two examples are shown in Fig. 2. Figure 2a shows type-C whiskers growing out of the positive pyramid

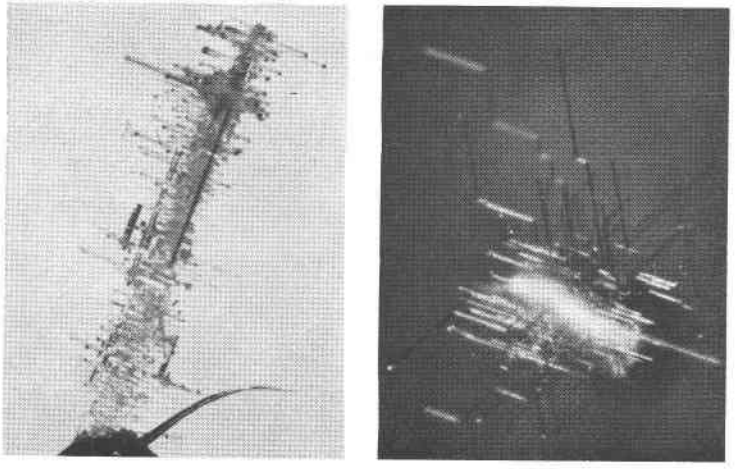

(a) (b)

FIG. 1. (a) A tree-like cluster of whiskers showing branching of A2 whiskers to form type-C whiskers and vice versa. This complex array of fibers has only one crystallographic orientation as indicated by x-ray diffraction. 70×. (b) A tree-like cluster of fibers viewed in the $[00\cdot1]^*$ direction. Many 60° kinks of type-A2 whiskers are present but no 30° kinks to type-A1 whiskers are observable. 70×.

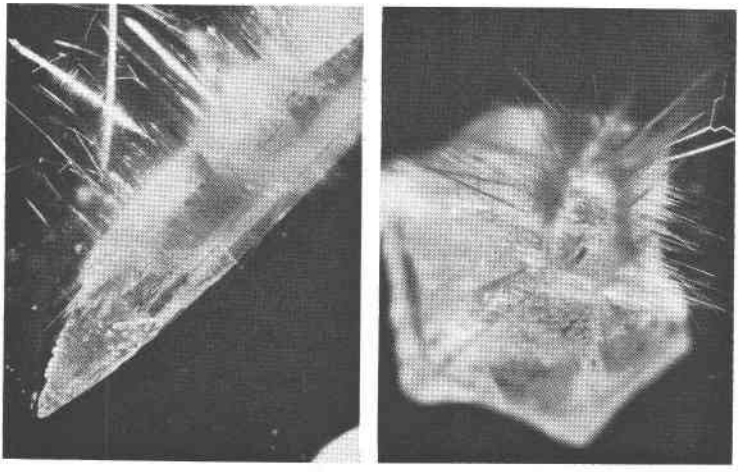

FIG. 2. (a) Overgrowth of BeO whiskers on a single crystal prismatic substrate. Two types of whiskers are observed: type-C fibers growing out of the positive pyramid $\{10\cdot1\}$, and type-A2 fibers growing from the positive pyramid and the prism $\{10\cdot0\}$. 10×. (b) Overgrowth of BeO whiskers on a single crystal pyramidal substrate containing an axial cavity. Growth occurs in six equally spaced directions in the basal plane, *i.e.*, the $[1\bar{1}\cdot0]^*$ set.

{10·1}. At high magnifications these whiskers appear identical to other type-C whiskers. No cores or twisting were ever observed. Type-A2 whiskers are shown growing out of the {10·1} face in Fig. 2b. Notice that two sets of A2 whiskers are present on each pyramidal face. Examination at high magnification in the electron microscope does not reveal any evidence for cores or twisting, but kinks are observed.

The most interesting group of microcrystals from the standpoint of morphology was obtained by the oxidation of Be metal. All three types of whiskers are developed. In addition three general types of platelets were formed. The whiskers are identical in all observable features to those already described except that some of the type-C whiskers show some intricate branched crystals, as shown in Fig. 3. All the branches are type-C whiskers, however, and there appears to be no crystallographic relation between the secondary crystals and the central crystal. The

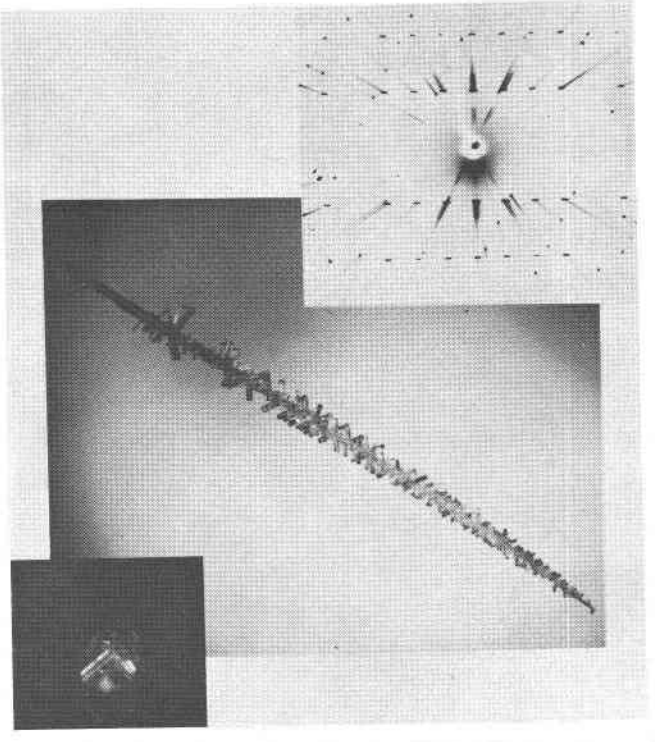

FIG. 3. A tree-like growth of a cluster of type-C whiskers. The insert *x*-ray diffraction pattern shows that the branches are type-C whiskers. In addition this pattern and the insert photograph viewed down the long axis of growth show that no crystallographic relationship exists between the secondary crystals and the central crystal. 10×.

secondary crystals fall into two categories, one group having the same cross-sectional dimensions as the central and a second group whose cross-sectional dimensions are much smaller than the central crystal. Both groups are present in Fig. 3.

Platelets are more common than whiskers in the experiment involving Be oxidation. These platelets may be classified by the two crystallographic vectors which define the plane of the platelet. Thus the three groups of platelets will be referred to as type C-A2, C-A1, and A1-A2, where the vectors have the same definitions as for the whiskers. Type-

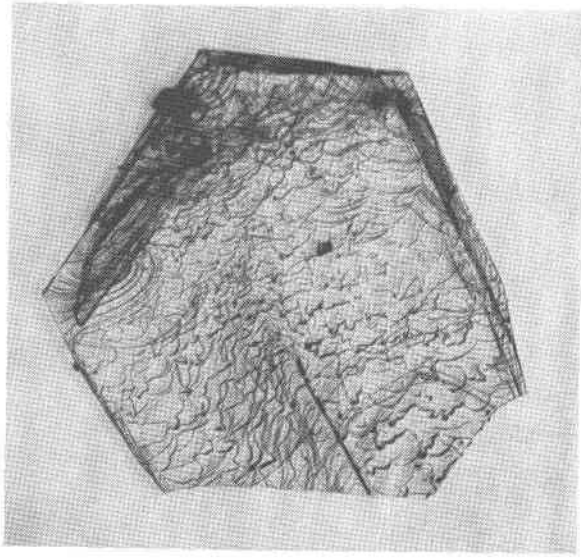

FIG. 4. A type-A1-A2 BeO platelet with the expected hexagonal outline. The intricate network of smooth growth spirals indicates normal growth and is not orientated in any particular crystallographic direction. The steps range in height from 500–2000 Å, depending on the particular region of the crystal face. Distorted steps demonstrate the effects of adsorbed impurities on the surface during growth. 10×.

A1-A2 platelets are rare. Platelets of this type, produced in a similar experiment, were also observed by Hessinger (private communication). The surface topography was studied by vapor coating the crystals with aluminum and examining the faces in reflected light using optical and multiple beam interferometric techniques. Figure 4 shows a typical example of the intricate network of growth layers that were observed. The steps bounding individual growth layers ranged in height from 500–2000 Å, depending on the particular region of the crystal face. In general, they are not parallel to crystal faces nor are they oriented in a

particular crystallographic direction. Instead they are clustered and arrayed in sweeping parallel curves. In some areas of the crystal, particularly where it appears that impurities are imbedded in the surface, the curves had jagged edges. Distorted growth steps are normally attributed to the effect of impurities. Impurities, absorbed and immobilized on the crystal surface, impede the flow of individual layers over the bounding surface, reduce the rate of layer generation and, consequently, the rate at which the crystal grows. The impurities apparently

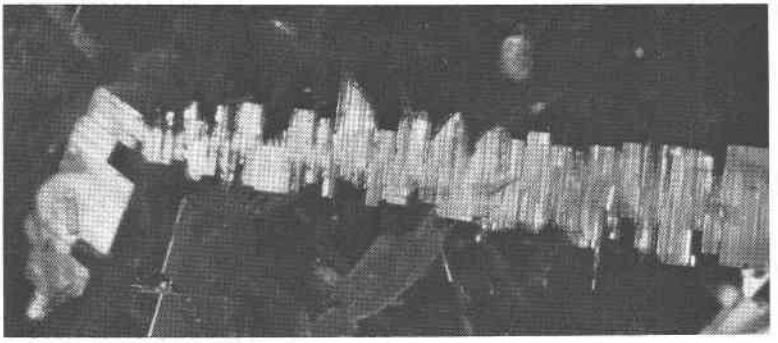

FIG. 5. A type-C-A2 platelet exhibiting a characteristic comb-like morphology. This complex morphology suggests the crystal was grown at very high growth rates. 10×.

become incorporated into the crystal as the steps move around or past them in the manner illustrated in Fig. 4.

Although most of the platelets formed by the oxidation of Be are rectangular, many of the crystals have very complex outlines. It is not uncommon for the platelets to branch, forming dihedral planes. Examples are shown in Figs. 5 and 6. Figure 5 shows a C-A2 type platelet exhibiting a comb-like effect which was relatively common.

Figure 6 shows a kinked plate and its respective x-ray precession pattern. Note that the crystal is single and is made up of platelets of both C-A1 and C-A2 types. The reflections on the x-ray pattern reflect the shape of the crystal so that it is easy to identify which part of the reflection is from which part of the crystal.

Twinning. Another feature of the microcrystals formed by the oxidation of Be is the presence of crystals which appear to be twinned. Figures 7 and 8 show two twinned crystals and their respective x-ray precession patterns. Close examination of the shapes of the diffracted spots identifies which half of the twin produces which pattern. The twins are identified by their twin planes which are (10·3) and (11·2), respectively, for Figs.

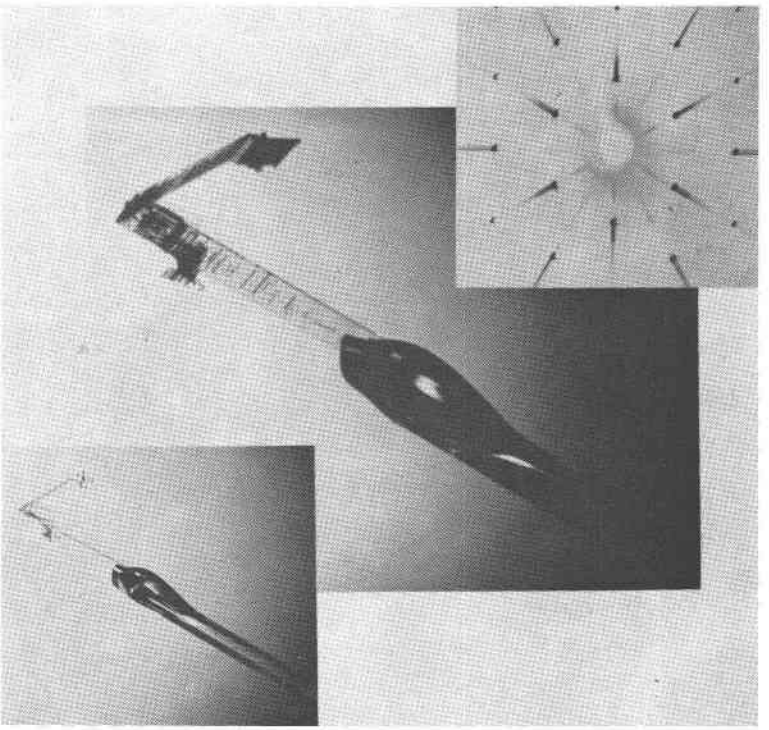

FIG. 6. Kinked BeO platelets formed by oxidation of Be. The right hand insert shows an x-ray diffraction pattern of the crystal along the line of intersection, while the left hand insert shows the 60° angle between the dihedral planes. The reflections of the x-ray pattern show the shape of the crystal and demonstrate that it is single and made up of type-C-A1 and C-A2 platelets. 70×.

7 and 8. Note that these are the reflections which are common to the two lattices in the respective patterns. Several examples of each twin were found in the batch of microcrystals; thus these twin types are felt to be well established.

Many other double crystals were found where two platelets joined at an edge, but no other twin types were positively identified. Only one other type of twin has been reported for BeO by Austerman (1963) and Smith, Newkirk, and Kahn (1964). In that twin the twin plane is (00·1) and the crystal reverses polarity in the two halves. This twin, discussed in detail in the following paper, cannot be verified without a polarity sensitive test such as etching or the development of pyramidal forms. No example was found among the microcrystals.

A few other twins have been reported for wurtzite-type compounds. Vom Rath (1871) reports the (80·9) and (00·1) twins and Cesaro (1895)

reports the (10·3) twin in ZnO. Merwin (1912) reports twinning on (10·2), (10·3), and (11·2) in CdS. Gindt and Kern (1958) report twinning on (10·3) and (10·2) in AlN.

Strength. Several type-C whiskers, grown by hydrolyzing BeF_2 vapor, were subjected to bending using a micromanipulator. Typical impurities and their concentrations for microcrystals of this type were aluminum, 10 ppm; magnesium, 10 ppm; lead, 800 ppm; others less than 10 ppm total. Figures 9a and b show a 0.018-cm-diameter-by-2.54-cm-long whisker be-

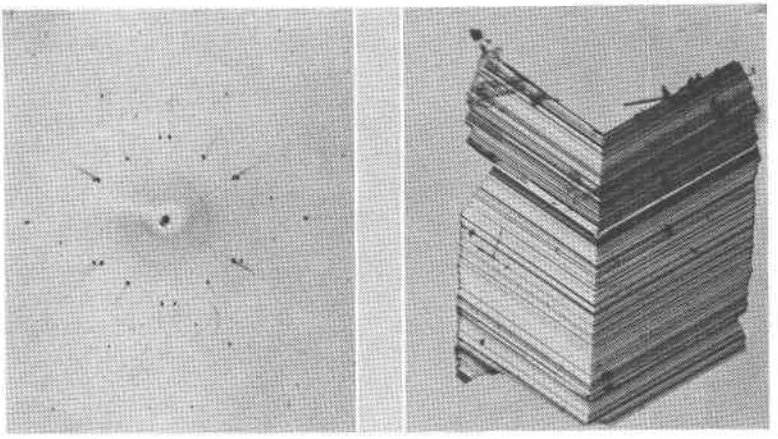

FIG. 7. The (10·3) twinned BeO platelets formed by oxidation of Be. On the left is the corresponding *x*-ray diffraction pattern. The shape of the reflection identifies which half of the crystal is responsible for each diffraction net. Note that the (10·3) reflections are common to each net and indicate the twin plane. This plane is also the composition plane as shown in the main photograph. Plane-polarized light, 70×.

fore and during a bending test. This particular whisker broke when bent 180°. However, smaller-diameter whiskers could actually be looped without breaking. No plastic deformation was observed prior to fracture. After fracture, both fragments were straight. Whiskers bent 270° and released returned to their original position.

The other fiber stress for a perfectly elastic body (Popov, 1952) is given by

$$\sigma_{max} = \frac{Er}{\rho} \tag{7}$$

where σ_{max} is the outer fiber tensile or compressive stress; E is Young's modulus of elasticity; r is the radius of the whisker; and ρ is the radius of curvature of the whisker when bent. For the present case, using $E = 60 \times 10^6$ lb/in^2, r = 0.0035 in, and $\rho = 0.0777$ in, the other fiber stress

is calculated to be 2,700,000 lb/in^2. The maximum strain is the ratio of whisker radius to radius of curvature, or 4.5%. These values are in close agreement with the value of 2,100,000 lb/in^2 determined by Budnikov and Shishkov (1961), 2,800,000 lb/in^2 reported by Ryschkewitch (1962), and the maximum of greater than 2% strain reported by Edwards and Happel (1963).

Now, for a perfect crystal, the maximum shear strength is $G/2\pi$, where

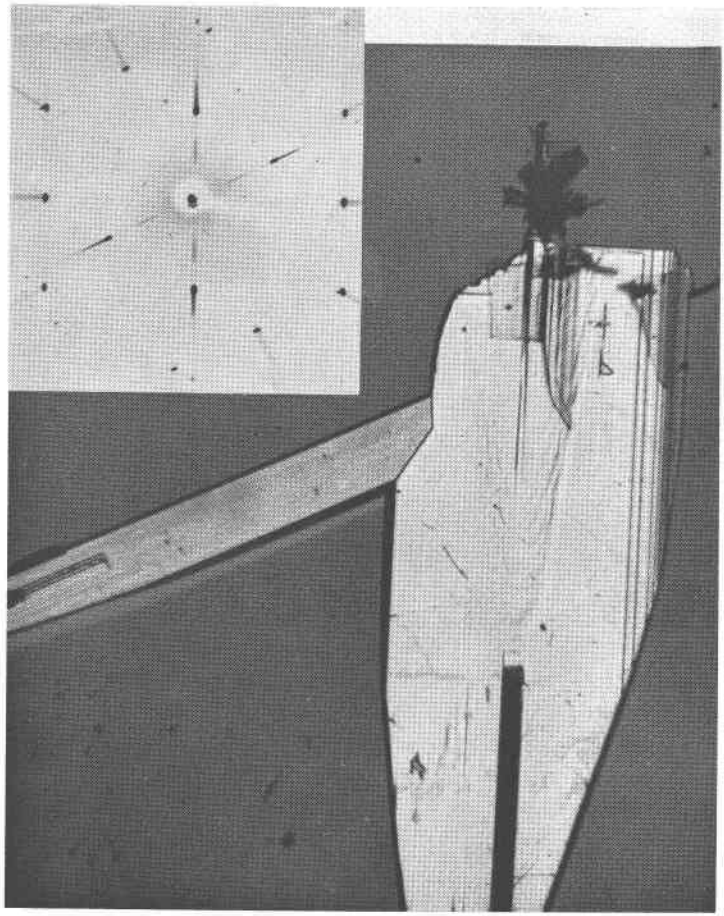

FIG. 8. The (11·2) twinned BeO platelet formed by oxidation of Be. The insert shows the corresponding x-ray diffraction pattern. As in Fig. 7, the corresponding nets of the pattern may be correlated to their respective sources. The (11·2) reflections are common and indicate that the twin plane is (11·2). Note that the composition plane is in part (11·2), but the other half of the boundary is of the type $(h_1h_1\cdot l_1)$-$(h_2h_2\cdot l_2)$. This crystal is the only example found with a composition plane different from the twin plane. Polarized light, 70×.

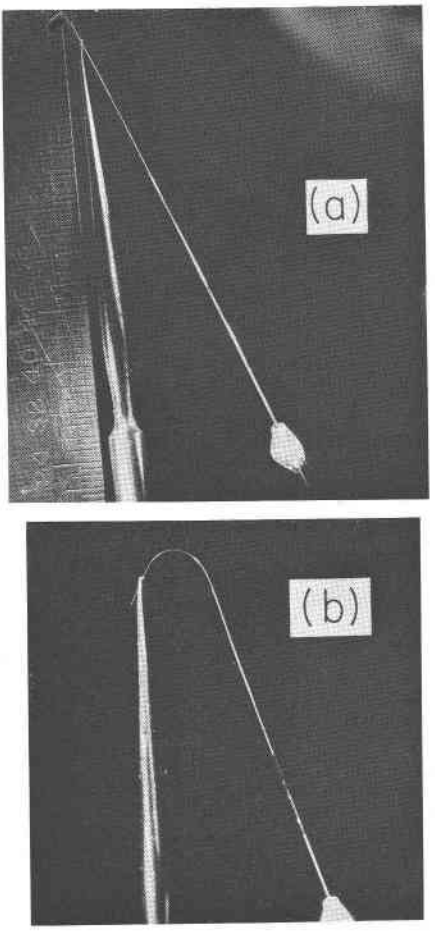

FIG. 9. Type-C whisker grown by hydrolyzing gaseous beryllium fluoride at elevated temperatures. (a) Before bending and (b) during a bending test. This particular whisker broke when bent close to 180°. Smaller diameter whiskers could actually be looped without breaking.

G is the shear modulus. Assuming BeO to be essentially isotropic and $G=23\times10^6$ lb/in^2, the maximum possible outer fiber stress is calculated to be 3.6×10^6 lb/in^2 in bending. Thus the measured strengths are near this maximum.

DISCUSSION

Growth features. While the normal whiskers and platelets have a wide variety of sizes and shapes, the principal growth directions were always found to be $[00\cdot1]$*, $[1\bar{1}\cdot0]$*, and, rarely, $[10\cdot0]$*, and the principal crystal

faces $\{00\cdot1\}$ pedions, the first order prism $\{10\cdot0\}$, and, occasionally, the second-order prism $\{11\cdot0\}$. Undoubtedly, the role of impurities is important in the nucleation and growth of microcrystals and macrocrystals. The presence of silicon in particular has been found to be extremely deleterious in that it causes spurious nucleation and inhibits overall growth rates. Where the substrate controls the growth direction, *i.e.*, in the oriented overgrowth on single macrocrystals, the predominance of only two growth directions is consistent with the theory of Frank (1953) and suggests the presence of well-behaved Burgers vectors in the substrate. The $[1\bar{1}\cdot0]$* directions lie along directions of closest packing in the BeO structure and are probable slip directions. The unit Burgers vector in this case would be pure screw and identical to the a-axis length of 2.698 Å (Bellamy *et al.* 1962). The $[00\cdot1]$* direction, however, is not a direction of close packing, but the unit Burgers vector can be pure screw with a magnitude of 4.377 Å. It would be expected that this Burgers vector would be operative during the growth of other wurtzite compounds for type-C whiskers such as reported for AlN (Kleber and Witzke, 1961; Evans and Davies, 1963; Drum, 1963) and ZnO (Struntz and Meldau, 1950). However, Drum (1963) reports that the type-C whiskers of AlN do not contain axial dislocations and probably do not grow by a dislocation mechanism. In contrast he reports type-A1 whiskers having axial dislocations with Burgers vectors a, although not all such whiskers contain dislocations. In contrast, a unit Burgers vector does not exist in the $[10\cdot0]$* direction, *i.e.*, this direction corresponds to half partials of the $[1\bar{1}\cdot0]$* directions. The fact that BeO microcrystals grow in this direction and in the $[30\cdot2]$ direction (Edwards and Happel, 1963) suggests either that other growth mechanisms are active or requires the presence of rather unusual Burgers vectors, *i.e.*, lattice translation vectors that are not minimum. Data in the literature on the formation of metal and other oxide microcrystals (Treuting and Arnold, 1957) indicate that growth does indeed occur preferentially in slip directions but that other growth directions are also possible. For example, Treuting and Arnold (1957) have reported tin whiskers growing in the $[10\cdot0]$* direction and AlN whiskers in the $[4\bar{2}\cdot3]$ direction (Drum, 1963). The latter AlN whiskers all have complicated axial defects, and evidently some dislocation mechanism is involved in their growth. Many contain c-Burgers vectors which surprisingly were not found in the type-C whiskers. Thus it appears that certain environmental conditions make each particular crystal growth system unique and complex and not subjected to rationalization by simple dislocation theory.

The complexity of the growth mechanisms in BeO is further illustrated by the complete lack of any measureable twist in these whiskers (Eshelby,

1953). If the whiskers contain a single axial screw dislocation with a prime Burgers vector equal to the cell constant, torsional strain of the whisker would be expected, as the following calculation illustrates. The lattice twist α per unit length is given by

$$\alpha(\xi) = \frac{b}{\pi R^2}(1 - \xi/R^2) \tag{8}$$

where b is the Burgers vector of the screw dislocation, R is the whisker radius, and ξ is the displacement of the dislocation from the whisker axis. Assuming the dislocation is at the center of the hexagonal cross section, the calculated twist for BeO whiskers with an effective radius of 1 μ is 5.7°/mm. This amount of twist should certainly be detectable by our x-ray diffraction techniques or optical measurements.

Data on the imperfections present in other microcrystalline materials are summarized in Table 1 and show that BeO is not unique in this absence of observable twists. The fact is that twisting and coring of whiskers is not common but is rare in most compounds. Only α-Al_2O_3 appears to be a well substantiated and reproducible example of whiskers showing twists. In this case, only type-C whiskers show the twists; types A1 and A2 do not twist and are not cored (Edwards and Happel, 1962). One cannot conclude, however, that the data are evidence for the complete absence of screw dislocations during growth in most systems. Lack of twisting could be explained by the interaction of parallel dislocations of opposite sign (Verma, 1953) or by dislocations being forced out of the whiskers to lateral surfaces by climb, slip, or point-defect trapping (Webb, 1962). Interestingly, many of the various types of whiskers had a small globule present at the tip during growth. This suggests that they may have grown by the (VLS) mechanism recently reported by Wagner and Ellis (1964). In this case, the liquid droplet, a solvent for BeO or $Be(OH)_2$ molecules, for example, molten beryllium, lead fluoride, beryllium fluoride, or calcium aluminum silicate, is a preferred site for deposition from the vapor. The whisker grows by precipitation of BeO from the saturated droplet and a screw dislocation is unnecessary. It appears, therefore, that an explanation of the processes which are important in the growth of BeO microcrystals must await the results of a detailed analysis of the defect substructure. One fact appears certain: the complexity of growth mechanisms in the laboratory is not present in nature. Schlichta (private communication) has observed twisting of whiskers in over 40 natural fibrous minerals of which chalcotrichite (Schlichta, 1957), cuprite, and pyrite are typical examples. It is interesting to note that in the 16th century natural fibrous minerals were the first whiskers observed and studied (Erker, 1574).

The growth of platelets, in contrast to the growth of whiskers, is even

TABLE 1. IMPERFECTIONS IN VARIOUS MICROCRYSTALLINE MATERIALS

Material	Observed lattice twist (degrees mm^{-1})	Axial core diameter (μ)	Burgers vector (Å)	Unit cell parameter, (Å)	Ref.
Zn	occasionally	none	0.77	2.664	Cabrera and Price (1958)
Sn	occasionally	none	$0.1b_0$–$10b_0$	6.64	Treuting and Arnold (1957)
Fe	—	none	—	2.8664	Schlichta (1958)
Cu	occasionally	none	mult. of b_0	3.6153	Schlichta (1958)
Ni	—	none	—	3.5238	Webb, *et al.*
Mn	—	none	—	8.912	Webb *et al.*
Ag	occasionally	none	mult. of b_0	4.0856	Webb *et al.*
Pd	occasionally	none	$1b_0$–$10b_0$	3.8902	Webb *et al.*
α Al_2O_3	0.045–5.62	0.1–1.0	13.0–130	13.0	Dragsdorf and Webb (1958)
BeO	none	none	—	4.3772	This work
ZnO	none	none	—	5.1948	Strunz and Meldau (1950)
Cu_2O	—	none	—	4.260	Schlichta (1957)
TiO_2 (rutile)	—	none	—	2.95	Schlichta (1957)
I SiC	—	yes	37.7	37.7	Verma (1951)
II SiC	—	yes	15.1	15.1	Verma (1951)
CuS	—	none	—	5.68	Schlichta (1957)
NaCl	occasionally	none	b_0–40 Å	5.62737	Webb (1958)
KI	occasionally	none	b_0–40 Å	7.052	Webb (1958)
AlN	none	none	—	4.965	Drum (1963)

less understood. A logical working hypothesis for future research would be to explain the observed growth features as resulting from the interaction of the active dislocation systems, namely, $[00\cdot1]^*$ and $[1\bar{1}\cdot0]^*$. The important parameters controlling the activation of one or the other or both of these systems would be the degree of supersaturation of the vapor phase, impurities, temperature gradient, etc. De Vries and Sears (1959) have already shown that variations in supersaturation can affect growth mechanisms and forms of crystals.

Twinning. The phenomenon of twinning in a crystal usually indicates that the lattice energy at the twin boundary is not much different from the lattice energy of the undisturbed structure. According to Read (1953) the boundary energy is composed of two contributions, the energy of disorder and the energy of elastic deformation. Thus a minimum state of

lattice energy implies a minimum amount of distortion in the bonding configuration across composition planes and no unsatisfied charges in the boundary region.

No theoretical treatment has been presented which will predict twinning in crystals. With our present state of knowledge it is possible only to analyze the observed twins and twin boundaries and attempt to correlate their occurrence with the twin boundary energy. Two twins have been observed in this study, one with a twin plane of $(11\cdot2)$ and one with $(10\cdot3)$ as the twin plane. The composition planes are identical with the twin planes except in the one crystal shown in Fig. 8.

The structure of the composition plane cannot be determined directly by any currently known method of analysis. Several possible configurations, however, may be deduced by attempting to fit the two halves of the twin keeping in mind the two requirements already mentioned. The only analysis of twinning in wurtzite-type structures has been made by Gindt and Kern (1958) for $(10\cdot3)$ and $(10\cdot2)$ twins in AlN. A fairly complete analysis of the (111) twins in silicon and germanium, which have the related sphalerite arrangement, has been made by Kohn (1958). Both of these studies have resulted in reasonable configurations in which the tetrahedral configurations show only minor distortions.

The wurtzite-type structure is polar which complicates the analysis of its twin boundaries. In general, in a structure, like BeO, where the oxygens dominate the packing, it is logical to assume that in the composition plane the oxygen atoms are very nearly continuous with both halves of the twin. In the $(11\cdot2)$ twin the oxygen arrangement which satisfies this requirement is shown in Fig. 10a projected along the direction $[1\bar{1}\cdot0]$*. Considering the polarity of the structure, three possible arrangements of the beryllium atoms exist depending on whether the polar axes are similar or opposed. The arrangement where the composition planes of the individuals are $(11\cdot\bar{2})$–$(11\cdot\bar{2})$ configurations are shown in Figs. 10b and c. Both of these configurations allow the coordination configurations to remain tetrahedral, although possibly with more distortion in the $(11\cdot2)$–$(11\cdot\bar{2})$ boundary. In the absence of etching studies on these crystals to determine the polarity relations, it is not possible to eliminate either of these boundary configurations. Possible computer solutions of the electrostatic lattice energy of the boundary structures will distinguish between these two possibilities. This approach is now being studied and will be the subject of a later paper.

The $(10\cdot3)$-type twin is even more difficult to analyze. Because of the lower symmetry of the projection of the structure along $[10\cdot0]$* when compared with the projection along $[1\bar{1}\cdot0]$*, several arrangements of the oxygen atoms are possible which allow some of the oxygens in the com-

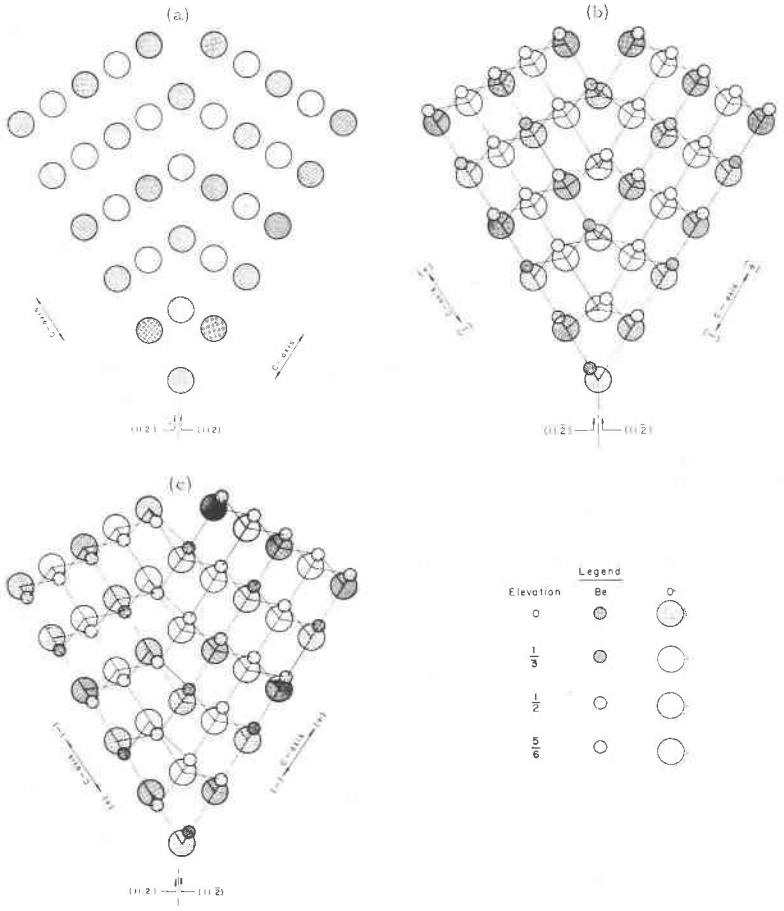

FIG. 10. Possible structural arrangements across the composition plane in the (11·2) twin. (a) The arrangement of oxygens which allows the atoms in the composition plane to be common to both halves of the twin. (b) and (c) Two arrangements of beryllium based on the oxygen arrangement in (a) which permit the tetrahedral coordination polyhedra to be maintained with a minimum of distortion.

position plane to be common to both halves of the twin. These arrangements are shown in Figs. 11a, b, and c. The first two are symmetrical about the twin plane. Where the composition and twin plane are identical, the plane should reflect one half into the other. This condition will lead to a minimum lattice energy for each half and consequently for the twin boundary as a whole. If the polarities of the halves are opposed, this requirement need no longer hold.

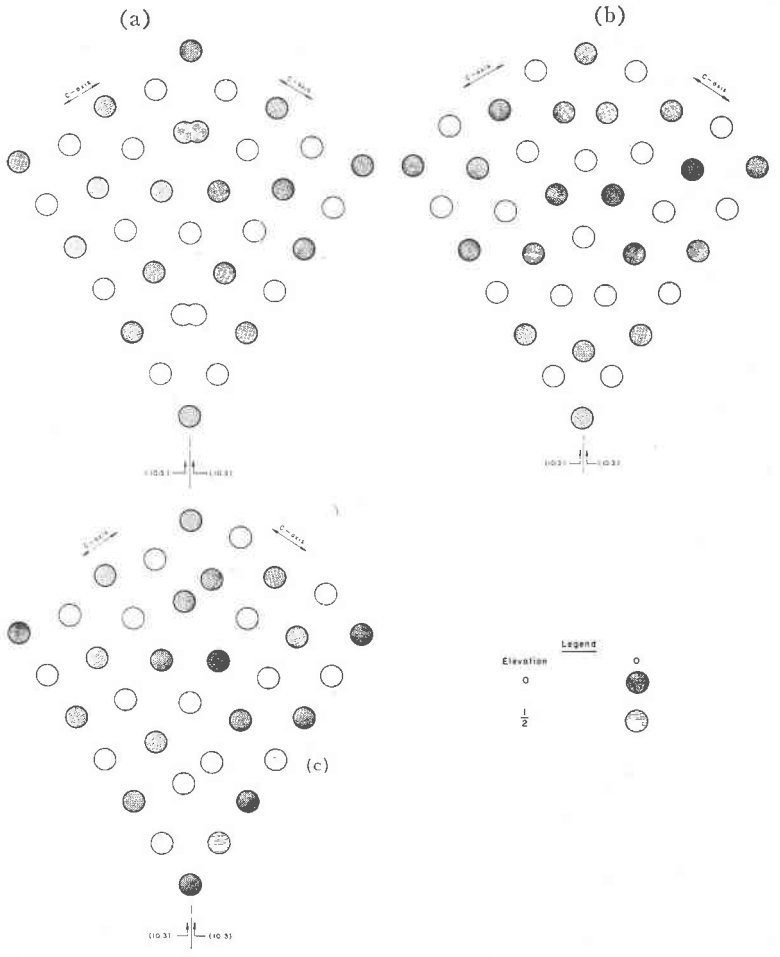

FIG. 11. Three possible oxygen arrangements across the composition plane in the (10·3) twin which allow atoms in the composition plane to be common to both halves of the twin. Note that the arrangements in (a) and (b) are symmetrical about the composition plane whereas the arrangement in (c) is not.

Based on these three oxygen arrangements, the consideration of polarity results in no less than ten possible boundary arrangements. Most of these arrangements lead to very irregular bonding configurations which do not allow the four-fold coordination to be maintained. Two arrangements, which are shown in Figs. 12a and b, do allow the four-fold coordination to be maintained except for one oxygen pair which shows three-fold coordination. In each of these arrangements the polarities of the

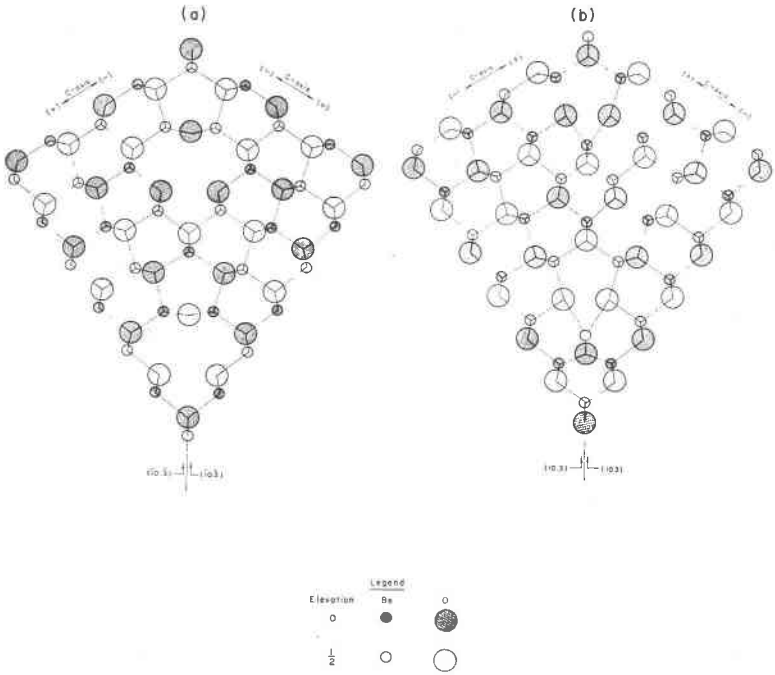

FIG. 12. The two most plausible arrangements of beryllium atoms based on the oxygen arrangements shown in Fig. 11a and b. In both arrangements the four-fold coordination is maintained with the exception of two pairs of oxygens which show three-fold coordination. The arrangement (b) is essentially identical to the boundary configuration devised by Gindt and Kern (1958) except that it does not show as much distortion of the bonding.

halves are similar. The arrangement shown in Fig. 12b is the same as that presented by Gindt and Kern to explain the twin boundary. Their figure contains more distortion than is acceptable to satisfy the requirement of equal distribution of distortion energy between the two halves. Etching of this twin type reveals that the arrangement shown in Fig. 12b is the correct one. Similarly, Gindt and Kern were able to determine that the polarities were similar by etching the AlN crystals in fused Na_2CO_3.

Note that the crystal shown in Fig. 8 has a composition plane other than (11·2). No attempt will be made at this time to analyze the composition plane until the lattice energy calculations can be made.

Only in the case of the (10·3) twin does a rational growth mechanism suggest itself. It seems certain that this twinned platelet grew by a twin boundary growth mechanism similar to that described by Dawson (1952) for paraffin dendrites. The 120° re-entrant angle would be a favored site for deposition of BeO because of the high level of supersaturation existing

within this area. Thus, the occurrence of the indestructible step at the twin boundary greatly accelerates growth in the [10·3]* direction.

Mechanical behavior of whiskers. In addition to growth features and twinning phenomenon, another basis for interest in BeO microcrystals is the exceptional strengths and elasticity observed in a material that is gen-

TABLE 2. RESULTS OF ROOM TEMPERATURE BENDING TESTS ON VARIOUS NONMETALLIC MICROCRYSTALS

Material	Calculated strength (psi)	Observed strain (%)	Young's modulus (10^6 psi)	Ref.
BeO	$2.1–2.8\times10^6$	4.5	60	Budnikov and Shishkov (1961)
MgO	3.5×10^6	—	42	Hulse (1961)
α-Al_2O_3	1.7×10^6	2.3	74	Webb and Forgeng (1958)
SiO_2	3.5×10^6	—	14	Gilman (1962)
Cu_3O_4	9.7×10^4	0.335	29	Webb *et al.*
Si_3N_4	4.6×10^5	4.0	12	Webb *et al.*
Cu_2N	—	5.8	—	Webb *et al.*
Fe_3C	1.2×10^6	4.7	25	Webb *et al.*
Mn_5Si_3	—	2.7	—	Webb *et al.*

erally considered to be relatively weak and brittle. Herring and Galt (1952) first observed strengths approaching the theoretical value in tin whiskers. They suggested that these strengths were attained "either because they are free of dislocations or because the few dislocations present cannot multiply sufficiently to give an observable amount of slip." Table 2 summarizes the results of bending tests on a variety of nonmetallic whiskers. The data show that the strengths for BeO whiskers are of comparable magnitude. The values are about 100 times greater than the highest strengths measured for polycrystalline BeO ceramics which are normally 30–60,000 psi. In addition, the results have practical implications in the field of composite materials and suggest the use of BeO whiskers as reinforcing agents whenever adequate and nondestructive bonding with the matrix can be attained. The ease with which copious quantities of whiskers were obtained in the presence of PbF_2 indicates that this process would be ideal for scale-up to pilot plant production. However, the temperature dependence of the strength of the whiskers and the effect of bonding on the mechanical properties of the whiskers must be determined before serious thought is given to fabricating composites.

Acknowledgments

The authors wish to acknowledge the assistance of W. Wadleigh and F. Berting in examining the microcrystals using the electron microscope, J. S. Kahn for petrographic examination of some of the reaction products, and D. K. Kingman and C. W. Griffith for running many of the growth experiments. We are indebted to P. L. Edwards, C. M. Drum, P. J. Schlichta, W. W. Webb, and A. Pabst for discussions pertaining to whisker growth and twinning phenomena.

References

Austerman, S. B. (1963) Growth of beryllia single crystals. *Jour. Am. Ceram. Soc.* **46,** 6–10.

Bellamy, B., T. W. Baker and D. T. Livey (1962) The lattice parameter and density of beryllium oxide determined by precise x-ray methods. *Jour. Nucl. Mat.* **6,** 1–4.

Budnikov, P. P. and N. V. Shishkov (1961) Some observations on the crystallization of beryllium oxide from the gas phase. *Dokl. Akad. Nauk. SSSR,* **138,** 1093.

Cabrera, N. and P. B. Price (1958) in *Growth and Perfection of Crystals.* John Wiley & Sons, Inc., New York, p. 206.

Cesaro, P. (1895). *Zeit. Krist.* **24,** 618–624.

Dawson, I. M. (1952) The study of crystal growth with the electron microscope II. The observation of growth steps in the paraffin n-hectane. *Proc. Roy. Soc.* **A 214,** 72–79.

DeVries, R. C. and C. W. Sears (1959) Growth of aluminum oxide whiskers by vapor deposition. *Jour. Chem. Phys.* **31,** 1256–1257.

Dragsdorf, R. G. and W. W. Webb (1958) Detection of screw dislocations in α-Al_2O_3 whiskers. *Jour. Appl. Phys.* **29,** 817–819.

Drum, C. M. Axial dislocations in thin ribbons of aluminum nitride. *Am. Phys. Soc. Meet.,* St. Louis, Mo., March 1963, *Paper* **FA8.**

Edwards, P. L. and R. J. Happel, Jr. (1962) Alumina whisker growth on a single-crystal alumina substrate. *Jour. Appl. Phys.* **33,** 826–827.

——— and R. J. Happel, Jr. (1963) Beryllium oxide whiskers and platelets. *Jour. Appl. Phys.* **33,** 943–948.

Erker, L. (1574) *Treatise on Ores and Assaying* [Engl. transl. by A. G. Siso and C. S. Smith, Univ. Chicago, 1951].

Eshelby, J. D. (1953) Screw dislocations in thin rods. *Jour. Appl. Phys.* **24,** 176–179.

Evans, P. E. and T. J. Davies (1963) Aluminum nitride whiskers. *Nature,* **197,** 587.

Frank, F. C. (1953) On tin whiskers. *Phil. Mag.* **44,** 854–860.

Gilman, J. J. (1962) Strength of ceramic crystals. *64th Ann. Meet. Am. Ceram. Soc.*

Gindt, R. and R. Kern (1958) ———. *Soc. Franc. Mineral. Cristall. Bull.* **81,** 266–273.

Herring, C. and J. K. Galt (1952) Elastic and plastic properties of very small metal specimens. *Phys. Rev.* **85,** 1060–1061.

Hessinger, P. (1962) (priv. comm.). See also U. S. Patent No. 3,125,416, March 17, 1964. Method for producing high-purity monocrystalline beryllia fibers and platelets.

Hulse, C. O. (1961) Formation and strength of magnesia whiskers. *Jour. Am. Ceram. Soc.* **44,** 572–575.

Kleber, W. and H. D. Witzke (1961) Growth and morphology of aluminum nitride single crystals. *Zeit. Krist.* **116,** 126–133.

Kohn, J. A. (1958) Twinning in diamond-type structures: a proposed boundary-structure model. *Am. Mineral.* **43,** 263–284.

LASKO, W. R. AND W. K. TICE (1962) Electron microscope investigation of extinction line contours in copper oxide whiskers. *Jour. Appl. Phys.* **33,** 2045–2050.

MERWIN, J. (1912) ———. *Am. J. Sci.* **34,** 341–344.

POPOV, E. P. (1952) *Mechanics of Materials.* Prentice-Hall, Inc., Englewood Cliffs, New Jersey, 97.

READ, W. T., JR. (1953) *Dislocations in Crystals.* McGraw-Hill Book Co., Inc., New York, 159.

RYSCHKEWITCH, E. (1962) Metal-oxide ceramics. *Inter. Sci. Tech.*, Feb., 1962, 54–61.

SCHLICHTA, P. J. (1957) Torsional strain of whiskers. *Am. Phys. Soc. Meet.*, Notre Dame, Indiana, June, 1957, *Paper* **H7.**

——— (1958) in *Growth and Perfection of Crystals.* John Wiley & Sons, Inc., New York, 214.

——— (1962) (priv. comm.).

SCOTT, V. D. (1959) Structure and growth of beryllium oxide on single crystals of beryllium. *Acta Cryst.* **12,** 136.

SMITH, D. K., H. W. NEWKIRK AND J. S. KAHN (1962) Crystal structure and polarity of beryllium oxide. *Jour. Electrochem. Soc.* **111,** 78–87.

STRUNZ, H. AND R. MELDAU (1950) Microscopic investigation of zinc oxide; investigation of ultramicromorphology. *Heidelberger Beitr. Mineral. Petrog.* **2,** 216–234.

TREUTING, R. G. AND S. M. ARNOLD (1957) Torsional strain and the screw dislocation in whisker crystals. *Acta Met.* **5,** 173–175.

VERMA, A. R. (1951) Spiral growth on carborundum crystal faces. *Nature,* **167,** 939.

——— (1953) *Crystal Growth and Dislocations.* Butterworth & Company, London.

VON RATH, A. (1871) Twinning of ZnO. *Ann. Phys.* **144,** 580–584.

WAGNER, R. S. AND ELLIS, W. C. (1964), Vapor-liquid-solid mechanism of single crystal growth. *Applied Physics Letters* **4**(5), 89–90.

WEBB, W. W. (1958) in *Growth and Perfection of Crystals.* John Wiley & Sons, Inc., New York, 230.

——— (1962) Point defect trapping in crystal growth. *Jour. Appl. Phys.* **33,** 1961–1971.

———, R. D. DRAGSDORF AND W. D. FORGENG (1957) Dislocations in whiskers. *Phys. Rev.* **108,** 498–499.

Manuscript received, March 10, 1964; accepted for publication, April 28, 1964.